Journal of Mathematical Chemistry Vol. 28, Nos. 1–3, 2000

Analysis of the electrolyte diode. Electro-diffusion and chemical reaction within a hydrogel reactor

J.H. Merkin [a], P.L. Simon [b] and Z. Noszticzius [b]

[a] *Department of Applied Mathematics, University of Leeds, Leeds, LS2 9JT, UK*
E-mail: amtjhm@amsta.leeds.ac.uk
[b] *Department of Chemical Physics, Technical University of Budapest, H-1521, Budapest, Hungary*
E-mail: {simonp,noszti}@phy.bme.hu

Received 11 July 2000

A reaction–diffusion system describing the electrolyte diode is investigated. This consists of a chemically crosslinked polyvinylalcohol (PVA) hydrogel cylinder in which a pH gradient is provided by having an acid and a base maintained at constant concentrations in reservoirs at each end of the one-dimensional reactor. A potential difference of a given strength is also applied across the gel cylinder. Previous experimental studies of the current–voltage characteristics (CVC) have shown two distinct cases, depending on whether a positive or negative potential difference was applied. The slopes of the linear current–voltage response curve are substantially different in the two cases, that in the 'forward' case being typically several orders of magnitude greater than that in the 'backward' case. Thus the system behaves like a semiconductor diode. The stationary concentration distribution for the different ions is described by a system of reaction–diffusion equations involving migration caused by the electric field. An approximate solution of these equations, using a simplified model, is presented and compared with results obtained by solving the full system numerically. The concentration profiles obtained from the numerical solution confirm the validity of the simplified model.

KEY WORDS: electrolyte diode, reaction–diffusion, electro-diffusion, Nernst–Planck equations

AMS subject classification: 92E20, 80A32

1. Introduction

Hydrogel reactors are used extensively to study the complex spatial and spatio-temporal structures that can arise in chemical systems. These reactors, so called CFURs (continuously fed unstirred reactors), developed initially in Texas [1,3] and Bordeaux [2], were constructed originally to study reaction–diffusion systems, especially chemical waves and Turing structures in a medium free of convection. They have subsequently proved to be an extremely versatile experimental procedure and have been used to show

0259-9791/00/1200-0043$18.00/0

that chemical systems, appropriately arranged, can sustain a wide variety of patterning processes. Much of this work is reviewed in [4,5].

A new version of this reactor, in which gradients of electrical potential as well as concentration gradients can be maintained, has been devised recently by Noszticzius and co-workers [6–8]. The main part of this reactor consists of a chemically crosslinked polyvinylalcohol (PVA) hydrogel cylinder in which a pH gradient is provided by having an acid and a base maintained at constant concentrations in reservoirs at each end of the one-dimensional reactor, HCl and KOH being used in the experiments. A potential difference of a given strength is also applied across the gel cylinder. The acid and base dissociate into their respective ionic components, specfically H^+, OH^-, Cl^- and K^+. These components diffuse and migrate under the action of the applied electric field, producing an electric current within the reactor. The experimental results are presented in terms of the dependence of this current on the applied potential difference.

The experiments [6] were performed specifically with HCl and KOH having equal concentrations c_0 in their respective reservoirs at the ends of the reactor (with a zero concentration of the other reactant also being maintained there). Two distinct cases were seen, depending on whether a positive or negative potential difference was applied. In the 'forward' case the electric field was applied so that it is the K^+ and Cl^- ions from the KOH and HCl solutions that migrate through the reactor, where they form a KCl solution, at concentration c_0. In the 'backward' case the tendency is for the OH^- and H^+ ions (from the KOH and HCl solutions respectively) to migrate into the reactor. In both cases, a linear current–voltage response curve is seen for sufficiently large applied voltages. However, the slopes of these curves are substantially different in the two cases, that in the 'forward' case being typically several orders of magnitude greater than that in the 'backward' case. Thus the system behaves like a semiconductor diode.

One reason suggested for this marked difference between the two cases is that, in the 'forward' case, the current is carried mostly by the K^+ and Cl^- ions (with the contribution from the H^+ and OH^- ions being negligible). These ions achieve the constant concentration c_0 throughout most of the reactor gel, which consequently has a relatively low impedance. In the 'backward' case, the applied electric potential is such that the K^+ and Cl^- ions cannot migrate far from their respective ends. The H^+ and OH^- ions are now the ones that are "pulled" into the reactor under the effect of the electric field, where they react to form a zone of pure water. This zone, where there are only low concentrations of H^+ and OH^- ions because of the reaction between them, has a relatively high impedance and it is where the majority of the potential drop occurs. Thus relatively large voltages need to be applied to produce a significant current.

A theoretical explanation for these phenomena was proposed in [6] and [8]. The stationary concentration distribution for the different ions is described by a system of reaction–diffusion equations involving migration caused by the electric field. An approximate solution of these equations, using a simplified model, was presented in [6,8]. The basic assumption behind this model is that the reaction between the H^+ and OH^- ions takes place in very narrow reaction layer(s), negligible in extent compared to the total length of the reactor. Therefore, in the simplified description the one-dimensional

reactor is divided into three parts: an alkaline, an acidic and a neutral zone, where no reaction is assumed to take place. The thin reaction layers act as division points between these regions. The ionic currents can be determined separately in each zone and, to describe the whole system, we add the contributions from these zones (neglecting the thickness of the reaction layers). Using this simplified model, approximate formulas for the current–voltage characteristics (CVC) can be derived theoretically (see formulas (2.1) and (2.2) in [8]).

The purpose of this paper is to study numerically the original (not simplified) reaction–diffusion system. The concentration profiles obtained from the solutions for the full system confirm the validity of the simplified model for the 'forward' case and enable us to derive an improved version of the simplified model for the 'backward' case. The approximate formulas for the CVC derived from the simplified model are checked against values obtained from the full system. We start by describing our model.

2. Model

The starting point for deriving our model is the Nernst–Planck equations relating the flux J_i to the concentration c_i of the ith chemical species to gradients of concentration and electrical potential. These equations can be expressed in 1D geometry (which is what we consider) as (see [9,10], for example)

$$J_i = -D_i\left(\frac{\mathrm{d}c_i}{\mathrm{d}x} + \frac{F}{RT}z_i c_i \frac{\mathrm{d}\phi}{\mathrm{d}x}\right) \tag{1}$$

for each species. We label the ionic species by

$$A^- \equiv \mathrm{OH}^-,\ B^+ \equiv \mathrm{H}^+ \text{ (the reacting species) } U^+ \equiv \mathrm{K}^+,\ V^- \equiv \mathrm{Cl}^-.$$

In (1) x measures distance along the reactor (of length L), D_i and z_i are the diffusion coefficients and ionic charges ($z_A = z_V = -1$, $z_B = z_U = +1$), respectively, F and R are Faraday's and the gas constants, T is absolute temperature (taken as constant) and ϕ is the electrical potential.

The mass transport equations are then derived using the fluxes given in (1), the reaction

$$\mathrm{H}^+ + \mathrm{OH}^- \rightleftharpoons \mathrm{H_2O} \quad \text{rate: } \frac{\mathrm{d}[\mathrm{H}^+]}{\mathrm{d}t} = \frac{\mathrm{d}[\mathrm{OH}^-]}{\mathrm{d}t} = k_0\big(K - [\mathrm{H}^+][\mathrm{OH}^-]\big) \tag{2}$$

and the corresponding ionic charges, as

$$\begin{aligned} D_A\left(a' - \frac{F}{RT}a\phi'\right)' + k_0(K - ab) &= \dot{a}, \\ D_B\left(b' + \frac{F}{RT}b\phi'\right)' + k_0(K - ab) &= \dot{b}, \\ D_U\left(u' + \frac{F}{RT}u\phi'\right)' &= \dot{u}, \end{aligned} \tag{3}$$

$$D_V\left(v' - \frac{F}{RT}v\phi'\right)' = \dot{v},$$

where primes (dots) denote differentiation with respect to distance (time), and where a, b, u and v are the concentrations of A^-, B^+, U^+ and V^-, respectively. The system is completed by the local electroneutrality condition

$$b + u - a - v = 0. \tag{4}$$

Note that condition (4) is, in effect, a reduced form of Poisson's equation for the potential and is valid when the Debye length can be assumed small (as it is here).

The current i is related to the fluxes through

$$i = F(-J_A + J_B + J_U - J_V). \tag{5}$$

In a steady, 1D system the condition, from Maxwell's equations, that i be divergence-free means that i is a constant.

We start by making equations (3), (4) dimensionless by writing

$$\begin{aligned} &\bar{x} = \frac{x}{L}, \quad a = c_0\bar{a}, \quad b = c_0\bar{b}, \quad u = c_0\bar{u}, \quad v = c_0\bar{v}, \\ &\overline{\phi} = \frac{F}{RT}\phi, \quad i = \frac{FD_Ac_0}{L}I. \end{aligned} \tag{6}$$

We are further assuming a steady state configuration for the reactor. Applying (6) in equations (3) (for the steady state) gives the dimensionless version of our model as, on dropping the bars for convenience,

$$\begin{aligned} \left(a' - a\phi'\right)' + \alpha(\kappa - ab) &= 0, \\ \delta_B\left(b' + b\phi'\right)' + \alpha(\kappa - ab) &= 0, \\ \delta_U\left(u' + u\phi'\right)' &= 0, \\ \delta_V\left(v' - v\phi'\right)' &= 0, \end{aligned} \tag{7}$$

where

$$\delta_B = \frac{D_B}{D_A}, \qquad \delta_U = \frac{D_U}{D_A}, \qquad \delta_V = \frac{D_V}{D_A}$$

are the ratio of diffusion coefficients and where the dimensionless parameters α and κ are given by

$$\alpha = \frac{k_0c_0L^2}{D_A}, \qquad \kappa = \frac{K}{c_0^2}.$$

We can incorporate the (dimensionless) current I into the system using the approach suggested by Snita and Marek [11]. From the dimensionless versions of equations (1) and (5) and electroneutrality (4), we obtain

$$I = a'(1-\delta_V) - b'(\delta_B - \delta_V) - u'(\delta_U - \delta_V) - E\left(a(1-\delta_V) + b(\delta_B + \delta_V) + u(\delta_U + \delta_V)\right), \tag{8}$$

where $E = -\mathrm{d}\phi/\mathrm{d}x$ is the (dimensionless) electric field. Equation (8) allows E to be written in terms of I, with equations (7), now in terms of a, b, u, becoming

$$\begin{aligned} a'' + (aE)' + \alpha(\kappa - ab) &= 0, \\ \delta_B\big(b'' - (bE)'\big) + \alpha(\kappa - ab) &= 0, \\ \delta_U\big(u'' - (uE)'\big) &= 0, \end{aligned} \tag{9}$$

where E is given by

$$E = -\frac{\mathrm{d}\phi}{\mathrm{d}x} = \frac{I - a'(1-\delta_V) + b'(\delta_B - \delta_V) + u'(\delta_U - \delta_V)}{a(1-\delta_V) + b(\delta_B + \delta_V) + u(\delta_U + \delta_V)} \tag{10}$$

and where I is a constant (the current). v is then determined from (4).

The boundary conditions to be applied are (assuming equal concentrations of KOH and HCl in the reservoirs)

$$\begin{aligned} a = u = 1, \quad b = 0, \quad \phi = 0 \quad \text{on } x = 0, \\ a = u = 0, \quad b = 1, \quad \phi = \Phi \quad \text{on } x = 1, \end{aligned} \tag{11}$$

where the constant (dimensionless) potential difference Φ can be either positive or negative.

3. Numerical method

Problems with the iterative convergence of the numerical scheme were encountered when trying to solve the two-point boundary-value problem (7), (11) directly for the steady states using shooting methods. Hence, it was decided to adopt an alternative approach, which worked well in all the cases treated. The initial-value problem corresponding to equations (9) (along the lines of equations (3)), subject to boundary conditions (11) and taking prescribed profiles for a, b and u as initial conditions, was considered. The current I was fixed at a given value and the electric field was calculated from (10). An explicit scheme, based on the predictor–corrector method, was used to solve this initial-value problem numerically, integrating until a steady state was achieved (to at least 5 decimal places in all three variables at each grid point). From the steady state electric field $E(x)$, Φ was then calculated using

$$\Phi = -\int_0^1 E(x)\,\mathrm{d}x. \tag{12}$$

It was found that a steady state was achieved relatively quickly, thus enabling the CVC to be readily built up, for given values of the parameters δ_B, δ_U, δ_V, α and κ, over successive runs. For all the results presented below we took 200 spatial grid points across the reactor.

4. Simplified theoretical description

Here we obtain a solution of equations (4), (7), (11) when the reaction term is neglected. To determine the approximate formulas for our simplified models described below, we consider a reactor of (dimensionless) length d and take as boundary conditions $a = a_i$, $b = b_i$, $u = u_i$, $v = v_i$ ($i = 1, 2$) on $x = 0$ and $x = d$, respectively.

With $\alpha = 0$, equations (7) can be expressed as

$$\begin{aligned} a' - a\phi' &= -J_A, \\ \delta_B(b' + b\phi') &= -J_B, \\ \delta_U(u' + u\phi') &= -J_U, \\ \delta_V(v' - v\phi') &= -J_V, \end{aligned} \tag{13}$$

with the (dimensionless) current given in terms of the now dimensionless fluxes J_i as

$$I = J_B + J_U - J_A - J_V.$$

Adding equations (13) and using electronuetrality (4), ϕ' can be eliminated. Integrating the resulting equation and applying the new boundary conditions gives

$$a + b + u + v = 2C(x) = 2(a_1 + v_1)\left(1 + (\beta_0 - 1)\frac{x}{d}\right), \tag{14}$$

where

$$\beta_0 = \frac{a_2 + v_2}{a_1 + v_1} = \frac{b_2 + u_2}{b_1 + u_1}.$$

Electroneutrality then gives

$$a + v = b + u = C(x). \tag{15}$$

Also, from equations (4), (7), (14), we have that

$$\left[(a + b + u + v)\phi'\right]' = 0, \quad \text{i.e.,} \quad \left(C(x)\phi'\right)' = 0, \tag{16}$$

from which it follows, on applying the boundary conditions that $\phi = 0$ at $x = 0$ and $\phi = \Delta\phi$ at $x = d$, that

$$\phi = \frac{\Delta\phi \ln(1 + \gamma x)}{\ln(1 + \gamma d)}, \tag{17}$$

where $\gamma = (\beta_0 - 1)/d$ and $\gamma \neq 0$. For the case $\gamma = 0$, $\beta_0 = 1$ we obtain

$$\phi = \Delta\phi \frac{x}{d}. \tag{18}$$

If we now multiply each of the equations in (13) by e^{ϕ} or $e^{-\phi}$ as appropriate and integrate over the range 0 to d, we can obtain the fluxes as

$$\begin{aligned} J_A &= -\frac{a_2 e^{-\Delta\phi} - a_1}{D_-}, & J_B &= -\frac{\delta_B(b_2 e^{\Delta\phi} - b_1)}{D_+}, \\ J_U &= -\frac{\delta_U(u_2 e^{\Delta\phi} - u_1)}{D_+}, & J_V &= -\frac{\delta_V(v_2 e^{-\Delta\phi} - v_1)}{D_-}, \end{aligned} \tag{19}$$

where the denominators in (19) are

$$D_\pm = \int_0^d e^{\pm\phi(x)}\,dx.$$

Using the above expressions for $\phi(x)$ in $D_\pm$, the fluxes J_i $(i = A, B, U, V)$ can be evaluated and then using these in the expression for I gives

$$\begin{aligned} I = {} & \frac{(\beta_0 - 1)(1 - \Delta\phi/\ln\beta_0)(a_2 e^{-\Delta\phi} - a_1 + \delta_V(v_2 e^{-\Delta\phi} - v_1))}{d(\beta_0 e^{-\Delta\phi} - 1)} \\ & - \frac{(\beta_0 - 1)(1 + \Delta\phi/\ln\beta_0)(\delta_U(u_2 e^{\Delta\phi} - u_1) + \delta_B(b_2 e^{\Delta\phi} - b_1))}{d(\beta_0 e^{\Delta\phi} - 1)} \end{aligned} \tag{20}$$

for $\beta_0 \neq 1$. When $\beta_0 = 1$ $(\gamma = 0)$ we obtain the simpler expression

$$\begin{aligned} I = {} & \Delta\phi\left(\frac{(a_2 e^{-\Delta\phi} - a_1) + \delta_V(v_2 e^{-\Delta\phi} - v_1)}{d(1 - e^{-\Delta\phi})}\right) \\ & - \Delta\phi\left(\frac{\delta_U(u_2 e^{\Delta\phi} - u_1) + \delta_B(b_2 e^{\Delta\phi} - b_1)}{d(e^{\Delta\phi} - 1)}\right). \end{aligned} \tag{21}$$

We are now in a position to assess the significance of these results for the experimental measurements presented in [6–8]. However, before doing so we examine the values of the various dimensionless parameters appropriate to these experiments.

5. Parameter values

In the experiments, the concentration c_0 of KOH and HCl in the reservoirs can be changed for different runs (as well as the applied potential drop Φ). We need to be able to estimate the values of the dimensionless parameters α and κ appropriate to a given value of c_0. To calculate the constant K we note that, in chemical equilibrium,

$$k_0[H^+][OH^-] - k_-[H_2O] = 0, \quad \text{giving} \quad K = \frac{k_-[H_2O]}{k_0},$$

where k_0 and k_- are the forward and reverse rate constants in (2). Using $k_0 = 1.3 \times 10^{11}$ M^{-1} s^{-1}, $k_- = 2.4 \times 10^{-5}$ s^{-1} and the concentration of water as $[H_2O]$= 55.6 M, we obtain $K = 1.0 \times 10^{-14}$ M^2. For a given c_0, α and κ are related by

$$\kappa = \frac{K(k_0 L^2)^2}{(D_A \alpha)^2} = \frac{6.25 \times 10^{12}}{\alpha^2}, \tag{22}$$

on taking values $D_A = D_{OH} = 5.24 \times 10^{-5}$ $cm^2 s^{-1}$ and $L = 0.1$ cm for the reactor.

Values of c_0 ranging from $c_0 \simeq 10^{-7}$ M (the smallest it is reasonable to take experimentally) to $c_0 \simeq 0.1$ M are used, suggesting a range of α from 10^7 to 10^{12} as being pertinent to the experimental observations. To ease the computational problems caused by having extremely large values for α, we conentrate on two specific cases at the lower end of the α range, namely the cases

$$\text{(i) } \alpha = 10^7,\ \kappa = 0.0625\ \left(c_0 = 4 \times 10^{-7}\right),$$
$$\text{(ii) } \alpha = 10^8,\ \kappa = 6.25 \times 10^{-4}\ \left(c_0 = 4 \times 10^{-6}\right).$$

We show that our approximate formulas (derived below) are in excellent agreement with the numerical solutions for these two cases. This gives us confidence in assuming that these approximate formulas are reliable estimates for the CVC for the whole range of α (and κ) appropriate to the experiments.

The values of the diffusion coefficients given in [8] suggest taking values $\delta_B = 1.77$, $\delta_U = 0.39$ and $\delta_V = 0.37$.

6. Forward case

6.1. Simplified theory

In the 'forward' case Φ is negative (as set up in our model), giving positive values for I. In this case it is the K^+ and Cl^- ions that are attracted into the reactor by the applied electric field, the H^+ and OH^- ions remain close to their respective ends. Thus we expect reaction (2) between H^+ and OH^- not to occur within the reactor and the reaction-free description given above should present a reliable guide for the CVC. To obtain this we put $d = 1$, $\Delta\phi = \Phi$ in (21) and apply the boundary conditions (11), to get

$$I = \Phi \frac{(\delta_U + \delta_V - (1 + \delta_B)e^{\Phi})}{e^{\Phi} - 1}. \tag{23}$$

When Φ is large (and negative)

$$I \sim (\delta_U + \delta_V)|\Phi| = 0.76|\Phi| \quad \text{as } \Phi \to -\infty \tag{24}$$

giving a linear CVC when $|\Phi|$ is large. Formula (24) is equivalent to the approximate expression given in [6,8].

We now examine relationship (24) from numerical solutions of the full system (9)–(11), including the reaction term.

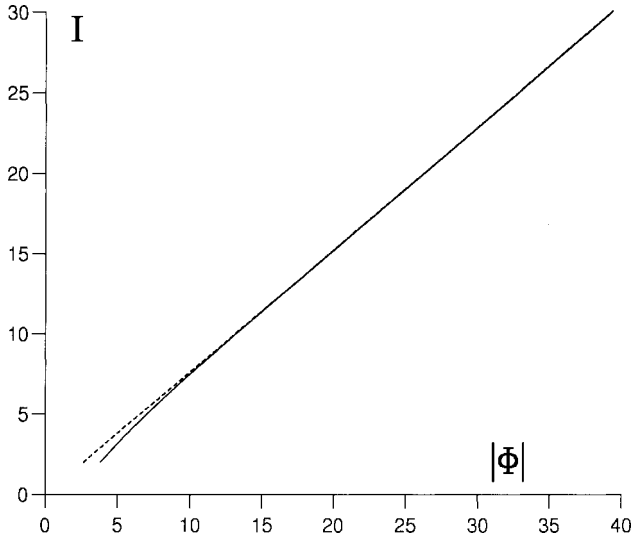

Figure 1. The current–voltage plot for the 'forward' case obtained from a numerical integration of the initial-value problem for $\alpha = 10^7$ ($\delta_B = 1.77$, $\delta_U = 0.39$, $\delta_V = 0.37$). Expression (24) is shown by the broken line.

6.2. Numerical results

The initial-value problem was solved numerically for a range of values of I until a steady state was achieved and the corresponding potential drop Φ calculated from (10), (12). Results for $\alpha = 10^7$ are shown in figure 1, with a plot of I against $|\Phi|$. Also shown in this figure (by the broken line) is expression (24) and we can see that there is excellent agreement between the numerical results and the analytic expression obtained from our simplified theory. The differences between the two sets of results occur at low I (or $|\Phi|$) where the simplified theory is not expected to be applicable.

The simplified approach requires that the system be essentially reaction-free, with OH^- and H^+ ions not penetrating far into the reactor. This can be seen in the profile plots in figure 2 (for $I = 20.0$, $\Phi = -26.324$). These plots are typical for the higher values of I (and $|\Phi|$) and show that the concentrations of K^+ and Cl^- are uniform over most of the length of the reactor, with the fall to zero concentrations at their respective ends being achieved in thin boundary-layer regions close to these ends. The concentrations of H^+ and OH^- both fall to zero rapidly in these boundary-layer regions.

The profiles shown in figure 2 justify our simplified model for the 'forward' case, which provides a reliable guide for calculating the CVC for the reactor in this case (see also figure 1). We now consider the 'backward' case.

7. Backward case

For this case I is negative, giving Φ positive, and it is now the OH^- and H^+ ions that are attracted into the reactor, with the K^+ and Cl^- ions remaining near their respec-

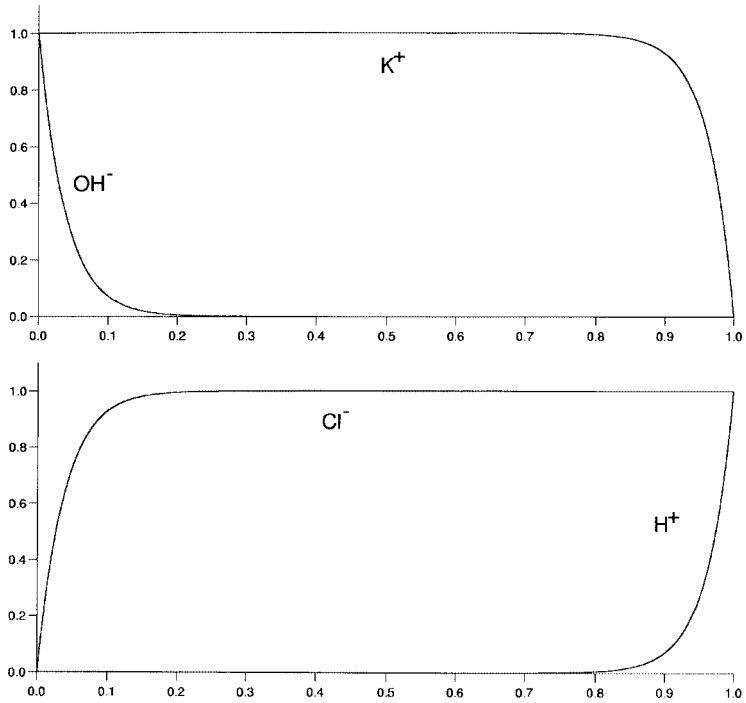

Figure 2. Concentration profiles for the 'forward' case obtained from a numerical integration of the initial-value problem for $I = 20.0$ ($\Phi = -26.324$), $\alpha = 10^7$ ($\delta_B = 1.77$, $\delta_U = 0.39$, $\delta_V = 0.37$).

tive ends. The OH^- and H^+ ions react (via (2)) in the central part of the reactor, forming a region of low ionic strength (neutral region) with a consequent large potential drop needed to maintain a given current. There will also be regions close to the ends of the reactor which contain either K^+ or Cl^- ions, the alkaline and acidic regions respectively. This is illustrated in figure 3 with typical profile plots for the 'backward' case, obtained from the numerical integration for $\alpha = 10^8$ and $I = -16.0$, ($\Phi = 159.1$). The three distinct concentration regions can clearly be seen in figures 3(a), (b). There is a high (negative) constant field E in the central region (figure 3(c)) giving the dominant part of the potential drop across the reactor. The reaction between OH^- and H^+ is confined to narrow regions at the junction between the different concentration regions (figure 3(d)). Note also the rapid fall in E within these reaction regions. The above considerations motivate us to construct a three-region model for the 'backward' case.

7.1. Simplified model

Our model consists of three separate (reaction-free) regions. There is a central (neutral) region, of extent d_1, in which there are only OH^- and H^+ ions present. This region is in chemical equilibrium which, with electroneutrality (4) and expressions (9),

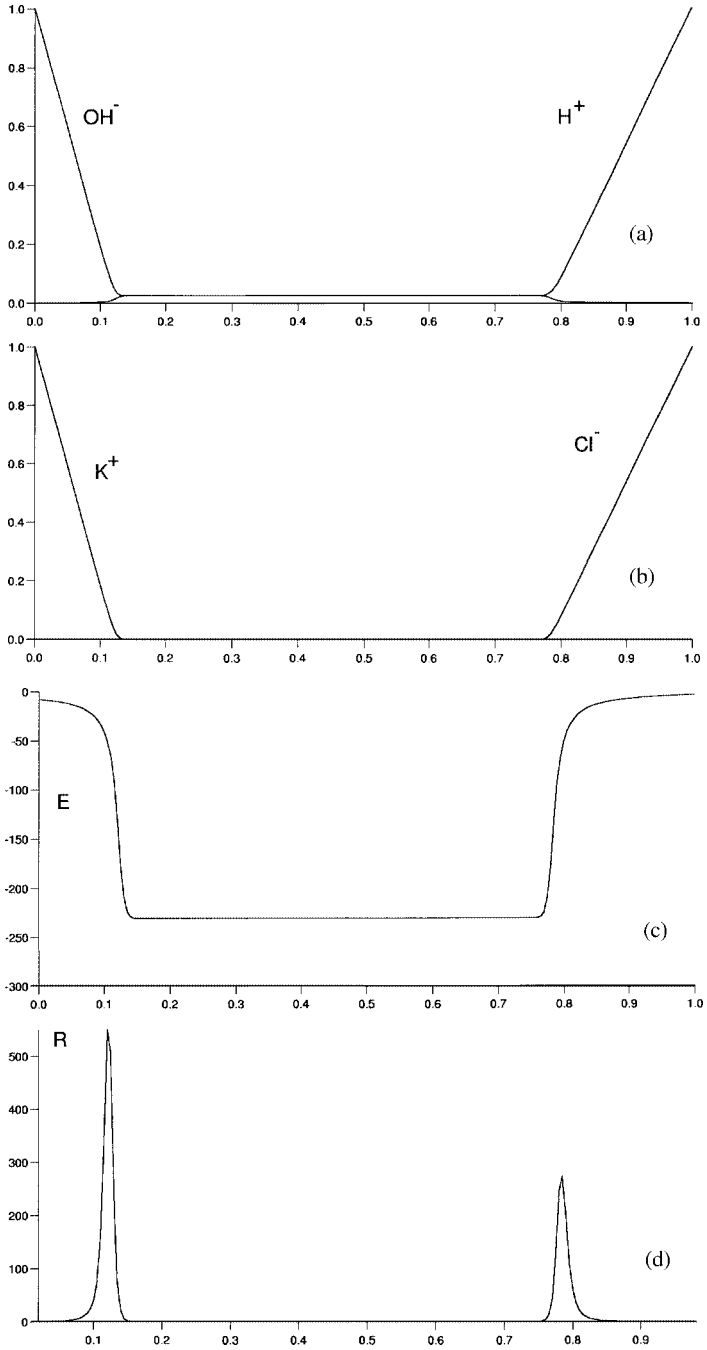

Figure 3. Concentration profiles for (a) $a \equiv[\mathrm{OH}^-]$, $b \equiv[\mathrm{H}^+]$, (b) $u \equiv[\mathrm{K}^+]$ and $v \equiv[\mathrm{Cl}^-]$, (c) the electric field E, and (d) reaction rate $R = \alpha(\kappa - ab)$ for the 'backward' case obtained from a numerical integration of the initial-value problem expression for $I = -16.0$ ($\Phi = 159.1$), $\alpha = 10^8$ ($\delta_B = 1.77$, $\delta_U = 0.39$, $\delta_V = 0.37$).

(10), gives

$$a = b = \sqrt{\kappa}, \qquad u = v = 0, \qquad E = \frac{I}{\sqrt{\kappa}(1+\delta_B)}. \tag{25}$$

The electric field is constant (and negative since I is) in this region, given by (25). The potential drop $\Delta\phi_1$ across the neutral region is then

$$\Delta\phi_1 = \frac{|I|d_1}{\sqrt{\kappa}(1+\delta_B)}. \tag{26}$$

There is a region close to the KOH reservoir (alkaline region) in which only K^+ and OH^- ions are present. The change in the concentration of b (H^+ ions) from $\sqrt{\kappa}$ in the central region to zero in the alkaline region is achieved in the narrow reaction zone between these two regions (see figure 3). From (14), (15), (17) we have

$$a = u = 1 + \gamma x, \quad b = v = 0, \quad \phi = \frac{\Delta\phi_2 \ln(1+\gamma x)}{\ln(1+\gamma d_2)}, \quad \text{where } \gamma = -\frac{(1-\sqrt{\kappa})}{d_2} \tag{27}$$

in the alkaline region, taking the potential drop across this region, of extent d_2, as $\Delta\phi_2$. We can calculate the (dimensionless) fluxes J_A and J_U from (19), or directly from (13) using (27), as

$$J_A = -\gamma\left(1 - \frac{\Delta\phi_2}{\ln(1+\gamma d_2)}\right), \qquad J_U = -\delta_U\gamma\left(1 + \frac{\Delta\phi_2}{\ln(1+\gamma d_2)}\right). \tag{28}$$

Since there is no K^+ in the central region and this species is not involved in the reaction, J_U must also be zero in the alkaline region, giving

$$\Delta\phi_2 = -\ln(1+\gamma d_2) = -\ln\sqrt{\kappa} \quad \text{and} \quad J_A = -2\gamma.$$

Then, since in this region $|I| = J_A = -2\gamma$, we obtain

$$d_2 = \frac{2(1-\sqrt{\kappa})}{|I|}. \tag{29}$$

The region close to the HCl reservoir (acidic region) has only H^+ and Cl^- ions. In this region, of extent $d_3 < x < 1$, we have, from (14), (15), (17),

$$\begin{aligned} &b = v = \left(\frac{1-\sqrt{\kappa}}{1-d_3}\right)\left(x - \frac{d_3-\sqrt{\kappa}}{1-\sqrt{\kappa}}\right), \qquad a = u = 0, \\ &\phi = -\frac{\Delta\phi_3}{\ln\sqrt{\kappa}}\ln\left(\frac{x-\bar{\gamma}}{d_3-\bar{\gamma}}\right), \quad \text{where } \bar{\gamma} = \frac{d_3-\sqrt{\kappa}}{1-\sqrt{\kappa}}, \end{aligned} \tag{30}$$

assuming a potential drop of $\Delta\phi_3$ across this region. The change in the concentration of a (OH^- ions) from $\sqrt{\kappa}$ in the central region to zero in the acidic region is achieved in

the narrow reaction zone between these two regions (again see figure 3). From (30) (or from (19)) we can calculate the fluxes J_B and J_V as

$$J_B = -\delta_B\left(\frac{1-\sqrt{\kappa}}{1-d_3}\right)\left(1-\frac{\Delta\phi_3}{\ln\sqrt{\kappa}}\right), \qquad J_U = -\delta_V\left(\frac{1-\sqrt{\kappa}}{1-d_3}\right)\left(1+\frac{\Delta\phi_3}{\ln\sqrt{\kappa}}\right). \quad (31)$$

Since there is no Cl^- in the central region and this species is not involved in the reaction, J_V must also be zero in the acidic region, giving

$$\Delta\phi_3 = -\ln\sqrt{\kappa} \quad \text{and} \quad J_B = -2\delta_B\left(\frac{1-\sqrt{\kappa}}{1-d_3}\right).$$

Since, in this region $|I| = -J_B$, we obtain

$$d_3 = 1 - \frac{2\delta_B(1-\sqrt{\kappa})}{|I|}. \quad (32)$$

Now $d_1 = d_3 - d_2$, and hence expressions (29), (32) give

$$d_1 = 1 - \frac{2(1+\delta_B)(1-\sqrt{\kappa})}{|I|}. \quad (33)$$

Assuming that the potential drop occurs only across the central region, expression (26) then gives

$$\Phi = \frac{|I| - 2(1+\delta_B)(1-\sqrt{\kappa})}{\sqrt{\kappa}(1+\delta_B)}, \quad (34)$$

from which we get the CVC

$$|I| = \sqrt{\kappa}(1+\delta_B)\Phi + 2(1+\delta_B)\big(1-\sqrt{\kappa}\big). \quad (35)$$

Similar approximate expressions were derived in [6,8]. The advantage of the present formulation is that the relationship between current and potential drop is in dimensionless form.

If we also include the potential drop across the alkaline and acidic regions, we add in a term $-2\ln\sqrt{\kappa}$ to the right hand side of (34), giving the slightly modified CVC

$$|I| = \sqrt{\kappa}(1+\delta_B)\big(\Phi + 2\ln\sqrt{\kappa}\big) + 2(1+\delta_B)\big(1-\sqrt{\kappa}\big). \quad (36)$$

We now examine the approximate form for the CVC (35), or its modified version (36), by comparing with numerical solutions of the initial-value problem.

7.2. Numerical results

Plots of the CVC for the $\alpha = 10^7$ and $\alpha = 10^8$ cases are shown in figure 4. In both cases there is a linear relationship between $|I|$ and Φ for reasonably large values with a slight variation from linear only at smaller values of $|I|$ (figure 4(a)). Results for specific examples are shown in table 1. Using these results we can calculate the linear slope S_B

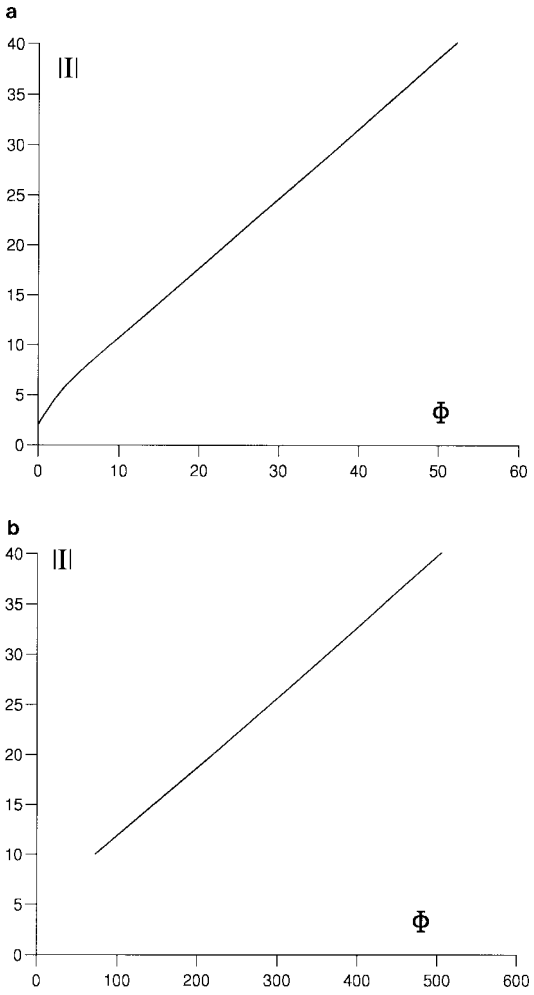

Figure 4. The current–voltage plot for the 'backward' case obtained from a numerical integration of the initial-value problem for (a) $\alpha = 10^7$, (b) $\alpha = 10^8$, with $\kappa = 6.25 \times 10^{12}\alpha^{-2}$, ($\delta_B = 1.77$, $\delta_U = 0.39$, $\delta_V = 0.37$).

Table 1
Potential drop Φ for the 'backward' case calculated from the numerical integrations for a given current I for a range of values of α, with $\kappa = 6.25 \times 10^{12}\alpha^{-2}$. Approximate values obtained from formulas (35) and (36) are also given, ($\delta_B = 1.77$, $\delta_U = 0.39$, $\delta_V = 0.37$).

α	I	Φ	From (35)	From (36)
10^7	20.0	23.391	22.881	25.653
10^7	40.0	52.309	51.762	54.534
10^8	20.0	220.25	210.8	218.2
10^8	40.0	506.13	499.6	507.0

of the CVC, $S_B = \Delta|I|/\Delta\Phi$, obtaining $S_B = 0.692$ and $S_B = 0.06996$, respectively. These are in good agreement with expression (35) (or (36)), which has

$$S_B = \sqrt{\kappa}(1 + \delta_B) = 6.925 \times 10^6 \alpha^{-1} \tag{37}$$

from (22). From this we can conclude that the simplified model predicts the slope of the CVC to a very good approximation.

The values obtained from expressions (35) and (36) are also given in table 1. These show that (35) gives a better approximation for the smaller values of α (and consequent larger values of κ). However, it is expression (36) which provides a better estimate for the more realistic larger values of α (and smaller κ). This might be expected, as the simplified model requires that the reaction zones be thin. A consideration of equations (9), in the limit of large α, suggests that the reaction zones are of thickness of $O(\alpha^{-1/3})$, thinning as α is increased (and κ decreased). This leads us to regard expression (36) as the more reliable guide to determine the CVC for the parameter ranges relevant to the experiments.

The approximate formulas for the CVC for the 'forward' (24) and 'backward' (36) cases show why there is a considerable difference in the slopes in the two cases. The slope S_F for the 'forward' case is $S_F = (\delta_U + \delta_V)$, here $= 0.76$, which is independent of α and κ and remains of $O(1)$ for all reservoir concentrations c_0. S_B depends strongly on α (and κ) from (37) decreasing with increasing α. It can become very small, of $O(10^{-5})$ or less, at the higher values of $\alpha \simeq 10^{12}$ corresponding to the higher values of reservoir concentrations c_0 used in the experiments.

8. Conclusions

We have solved numerically the reaction–diffusion system (7) describing the electrolyte diode and determined its current–voltage characteristics. Our results show (in qualitative agreement with the experiments) that the slope of the CVC in the 'forward' case is very much greater than that in the 'backward' case. We compared our numerical results with theoretical values obtained from a simplified approximate theory and found very good agreement between the two sets of results. The only differences between the two occurred at low voltages where the simplified theory is not expected to be applicable.

The concentration profiles obtained numerically confirm the simplifying assumptions of the approximate theory. In the 'forward' case (see figure 2) the concentrations of K^+ and Cl^- are uniform over most of the length of the reactor, with the fall to zero concentrations at their respective ends being achieved in thin boundary-layer regions close to these ends. The concentrations of H^+ and OH^- are significant only in their respective thin boundary-layer regions. Thus the capillary is filled almost entirely with KCl solution, as assumed in the simplified theory. In the 'backward' case three distinct concentration regions arise (clearly seen in figures 3(a), (b)) again in a good agreement with the assumptions of the simplified theory. There is a central (neutral) zone (of pure water) separating the alkaline and acidic regions. In these latter regions the KOH and

HCl concentrations fall linearly from their boundary values to virtually zero in the central zone. The reaction between OH^- and H^+ is confined to narrow layers at the two ends of the central zone at the junctions with the acidic and alkaline regions.

Acknowledgements

This work was partially supported by OTKA (F-022228, T-030110) and FKFP (0287/1997) grants. Co-operation of British and Hungarian authors was made possible by a grant from the British Council Hungarian–British Joint Academic and Research Programme and the ESF programme REACTOR.

References

[1] Z. Noszticzius, W. Horsthemke, W.D. McCormick, H.L. Swinney and W.Y. Tam, Sustained chemical waves in an annular gel reactor: a chemical pinwheel, Nature 329 (1987) 619–620.
[2] V. Castets, E. Dulos, J. Boissonade and P. De Kepper, Experimental evidence of a sustained standing Turing-type nonequilibrium chemical pattern, Phys. Rev. Lett. 64 (1990) 2953–2956.
[3] Q. Ouyang and H.L. Swinney, Transition from a uniform state to hexagonal and striped Turing patterns, Nature 352 (1991) 610–612.
[4] R. Kapral and K. Showalter, *Chemical Waves and Patterns* (Kluwer, Dordrecht, 1995).
[5] B.R. Johnson and S.K. Scott, New approaches to chemical patterns, Chem. Soc. Rev. 25 (1996) 265–273.
[6] L. Hegedus, M. Wittmann, N. Kirschner and Z. Noszticzius, Reaction, diffusion, electric conduction and determination of fixed ions in a hydrogel, Progr. Colloid. Polym. Sci. 102 (1996) 101–109.
[7] L. Hegedus, M. Wittmann, N. Kirschner and Z. Noszticzius, Electrolyte transistors: Ionic reaction–diffusion systems with amplifying properties, J. Phys. Chem. A 102 (1998) 6491–6497.
[8] L. Hegedus, N. Kirschner, M. Wittmann, P.L. Simon, Z. Noszticzius, T. Amemiya, T. Ohmori and T. Yamaguchi, Nonlinear effects of electrolyte diodes and transistors in a polymer gel medium, Chaos 9 (2) (1999) 283–297.
[9] I. Rubinstein, *Electro-Diffusion of Ions*, SIAM Studies in Applied Mathematics, Vol. 11 (Philadelphia, USA).
[10] J. Keener and J. Sneyd, *Mathematical Physiology*, Interdisciplinary Applied Mathematics, Vol. 8 (Springer-Verlag, New York, 1998).
[11] D. Snita and M. Marek, Transport and reaction in ionic chemical systems, Phys. D 75 (1994) 521–540.